

The Effect of Fluid Loading and Hypertonic Saline Solution on Cortical Cerebral Microcirculation and Glycocalyx Integrity

Vlasta Dostalova, MD, PhD,* David Astapenko, MD,* Vlasta Dostalova Jr,* Jaroslav Kraus,*
Vladimir Cerny, MD, PhD,*†‡§ Alena Ticha, RNDr, PhD,|| Radomir Hyspler, MD, PhD,||
Vera Radochova, DVM,¶|| Jiri Paral, MD, PhD,¶|| and Pavel Dostal, MD, PhD*

Background: Fluid loading and hyperosmolar solutions can modify the cortical brain microcirculation and the endothelial glycocalyx (EG). This study compared the short-term effects of liberal fluid loading with a restrictive fluid intake followed by osmotherapy with hypertonic saline (HTS) on cerebral cortical microcirculation and EG integrity in a rabbit craniotomy model.

Methods: The experimental rabbits were allocated randomly to receive either <2 mL/kg/h (group R, n=14) or 30 mL/kg/h (group L, n=14) of balanced isotonic fluids for 1 hour. Then, the animals were randomized to receive 5 mL/kg intravenous infusion of either 3.2% saline (group HTS, n=14) or 0.9% saline (group normal saline, n=13) in a 20-minute infusion. Microcirculation in the cerebral cortex based on sidestream dark-field imaging, a morphologic index of glycocalyx damage to sublingual

and cortical brain microcirculation (the perfused boundary region), and serum syndecan-1 levels were evaluated.

Results: Lower cortical brain perfused small vessel density ($P=0.0178$), perfused vessel density ($P=0.0286$), and total vessel density ($P=0.0447$) were observed in group L, compared with group R. No differences were observed between the HTS and normal saline groups after osmotherapy. Cerebral perfused boundary region values ($P=0.0692$) and hematocrit-corrected serum syndecan-1 levels ($P=0.0324$) tended to be higher in group L than in group R animals.

Conclusions: Liberal fluid loading was associated with altered cortical cerebral microcirculation and EG integrity parameters. The 3.2% saline treatment did not affect cortical cerebral microcirculation or EG integrity markers.

Key Words: brain, hypertonic saline, microcirculation, osmotherapy, glycocalyx

(*J Neurosurg Anesthesiol* 2018;00:000–000)

Received for publication February 26, 2018; accepted June 19, 2018.

From the Departments of *Anesthesiology and Intensive Care Medicine; ||Clinical Biochemistry, Faculty of Medicine Hradec Kralove, Charles University; §Department of Research and Development, University Hospital Hradec Kralove, Hradec Kralove; ‡Department of Anesthesiology, Perioperative Medicine and Intensive Care, J.E. Purkinje University, Masaryk Hospital, Usti nad Labem; ¶Department of Military Surgery, Faculty of Military Health Sciences, Hradec Kralove University of Defense, Brno, Czech Republic; and †Departments of Anaesthesia, Pain Management and Perioperative Medicine, Dalhousie University, Halifax, NS, Canada.

V.D.: conceived the study, performed the animal experiments, and prepared the manuscript. P.D.: participated in the experimental design, performed the statistical analysis, and finalized the manuscript. V.D. Jr: participated in the animal experiments, performed the SDF analysis, and facilitated manuscript drafting. J.P., V.C., and R.H.: participated in the study design and facilitated manuscript drafting. D.A., J.K., A.T., and V.R.: participated in the animal experiments and facilitated manuscript drafting.

Funded by the Ministry of Defense of the Czech Republic under the project “A Long-term Organization Development Plan 1011” and was also partially supported by the Ministry of Health of the Czech Republic, grant no. 15-31881A.

The authors have no conflicts of interest to disclose.

Address correspondence to: Pavel Dostal, MD, PhD, Department of Anesthesiology and Intensive Care Medicine, Faculty of Medicine Hradec Kralove, Charles University, University Hospital Hradec Kralove 53009, Hradec Kralove, Czech Republic (e-mail: pavel.dostal@fnhk.cz).

Copyright © 2018 Wolters Kluwer Health, Inc. All rights reserved.
DOI: 10.1097/ANA.0000000000000528

BACKGROUND

Fluid therapy is a fundamental component of the intraoperative management for neurosurgical patients. Perioperative fluid therapy can affect longer-term postoperative outcomes.¹ The volume of fluid administered during the perioperative period is dependent upon multiple factors, such as preoperative hydration, intraoperative blood loss, and hemodynamic stability, as well as the preferences of the anesthesiologist and surgeon.² However, accumulating evidence implies harmful effects from positive fluid balance and higher fluid intake, mainly in patients with a subarachnoid hemorrhage.³ Furthermore, goal-directed fluid restriction reduced the length of the intensive care unit stay in patients undergoing high-risk brain surgery, probably due to a lower incidence of respiratory complications.⁴ Moreover, fluid restriction can also modify the extent of edema at the surgical site, because overhydration and surgical trauma can cause endothelial dysfunction and interstitial edema.⁵

Local cerebral blood flow is regulated to meet neuronal metabolic demands under normal conditions, a mechanism known as neurovascular coupling that adapts the local flow to the rate of exchange of vital nutrients across the blood-brain

barrier (BBB).⁶⁻⁸ The BBB exerts its barrier function mainly by endothelial cells that are interconnected by tight junctions, and are surrounded by the basal lamina, pericytes, and astrocytes, forming a stabilizing network.⁷ Another significant barrier function is provided by the endothelial glycocalyx (EG).⁸ EG is a gel-like matrix that covers the luminal side of the endothelium. An intact EG reduces the interactions between the endothelium and blood components and plays an important role in flow regulation. Consequently, EG is a key regulator of vascular permeability, cerebral blood flow, capillary perfusion, and cell adhesion.⁸⁻¹¹ Severe damage to the glycocalyx is associated with increased BBB permeability, probably due to a loss of the negative EG charge and a local increase in inflammatory factors, such as matrix metalloproteinases and vascular endothelial growth factor, which disrupt the tight junctions and BBB hyperpermeability.¹² The EG can be damaged by several mechanisms and conditions, including fluid and salt overload.¹³⁻¹⁵

Hyperosmolar solutions are used during neurosurgical procedures to facilitate intraoperative brain relaxation, to improve operating conditions, and to prevent neurological deterioration. Intraoperative infusion of crystalloid solutions and the use of hyperosmolar solutions can modify cortical brain microcirculation and the EG.

Changes in microcirculation can be investigated using sidestream dark-field (SDF) imaging, a well-validated stroboscopic light-emitting diode ring-based imaging modality used in a clinical setting,¹⁶ and previously used to study changes in microcirculation under various clinical conditions in both animal¹⁷ and human studies.¹⁸ SDF has also been used to analyze cortical brain microcirculation in animals with different pathologic conditions, including sepsis.¹⁹⁻²² SDF technology has been recently used by our group to study the short-term effects of mannitol, hypertonic saline (HTS), and hypertonic lactate infusion on cortical microcirculation in rabbits.^{23,24}

Changes in the glycocalyx can also be monitored using biochemical or imaging methods.^{9,11} The circulating level of the cell surface heparan sulfate proteoglycan syndecan-1 is a commonly used biochemical marker of EG damage.^{9,11} The perfused boundary region (PBR) is a novel parameter that indirectly describes the degree of EG damage, signifying the number of penetrating red blood cells (RBCs) into the EG,^{9,11,25-27} which has been recently used for in vivo assessment of the human cerebrovascular glycocalyx.²⁸

The aim of the present study was to compare the short-term effects of restrictive infusion (R) with liberal fluid loading (L) of a balanced isotonic crystalloid solution on cerebral cortical microcirculation, and to compare the short-term effects of osmotherapy using HTS (with/without the R or L infusion strategy) on cerebral cortical microcirculation and EG integrity.

METHODS

Animals

All experimental procedures were performed after approval from the Animal Welfare Body of the University

of Defense, Faculty of Military Health Sciences in Hradec Kralove, the Czech Republic (approval no. 50-37/2016-6848), in accordance with Czech legislation on the protection of animals in compliance with the Directive 2010/63/EU of the European Parliament and Council. In total, 28 female rabbits (New Zealand white rabbits; weight: 2.6 to 3.0 kg; VELAZ 34081/2008-10001, CZ 21906828, Unetice, the Czech Republic) were included in the study. The animals were housed in a standard cage at 21°C under a 12-hour dark/12-hour light cycle with ad libitum access to laboratory chow and tap water. The rabbits were used for the study after a 1-week acclimatization period.

Anesthesia, Surgical Preparation, and Biochemical Analysis

After an overnight fast with unrestricted access to tap water, the rabbits were anesthetized using intramuscular induction doses of ketamine (15 mg/kg) and xylazine (3 mg/kg). The body locations used for cannulation, electrocardiogram electrodes, tracheostomy, and both the right and the left temporo-parieto-occipital areas of the head were shaved. The animals were placed in the supine position on an operating table; inhalation of 2 L/min of oxygen was started. Intravascular cannulas (Vasofix Safety, B. Braun, Melsungen, Germany) were inserted into both marginal ear veins (G24) and the right central ear artery (G22) for continuous blood pressure monitoring, arterial blood gas analysis, and intravenous infusion. Supported ventilation via a cone-shaped mask was started after intravenous induction with propofol (3 mg/kg, propofol 1% MCT/LCT Fresenius; Fresenius Kabi Deutschland GmbH, Bad Homburg, Germany), fentanyl (1 µg/kg, Fentanyl Torrex; Chiesi Pharmaceuticals GmbH, Vienna, Austria), muscle relaxation with pipecuronium bromide (0.6 mg/kg/h, Arduan; Gedeon Richter Plc., Budapest, Hungary), and inhalation of isoflurane via a mask (1.5 vol%, Forane; AbbVie Inc., Chicago, IL). The animals were tracheotomized, and a cuffless tracheal tube with an outer diameter of 3 mm was inserted, between the third and fourth tracheal rings. Mechanical ventilation was initiated using an anesthesia machine (Cirrus Trans 2/Vent 2; Datex, Helsinki, Finland) with initial settings of pressure-controlled ventilation, positive end-expiratory pressure of 3 cm H₂O (lowest value on the ventilator), respiratory rate of 40 breaths/min, and inspiratory pressure of 14 to 16 cm H₂O according to weight, and subsequently adjusted according to end-tidal carbon dioxide tension and the first blood gas analysis results. A baseline sample of arterial blood was sent to the laboratory to evaluate the level of blood gases, sodium, chloride, syndecan-1, and hemoglobin. Hemodynamic data were recorded, and baseline sublingual SDF imaging was performed. Mean arterial blood pressure was maintained at > 55 mm Hg with a norepinephrine infusion, as necessary. Mean arterial blood pressure, heart rate, and rectal temperature were recorded throughout the study. Temperature was maintained at 38.5 to 39.5°C using a heating pad and a thermoisolation blanket. Balanced anesthesia was maintained using isoflurane (0.6 to 1 vol%, Forane; AbbVie Inc.) in a mixture of 1 L/min oxygen and 1.2 L/min air with an inspiratory oxygen fraction of 50% to 55%, and intermittent fentanyl (1 µg/kg) and

pipecuronium bromide (0.5 mg/kg) boluses. Intravenous infusion of a balanced crystalloid solution was administered according to the experimental group.

After tracheostomy, each animal was rotated into the prone position. The skin and periosteum of the skull were incised and reflected; bleeding was contained by bipolar electrocoagulation. The margins of the exposed area were determined by the midline, the base of the right ear, the external occipital protuberance, and the right caudal supraorbital process. A 3 mm hole was drilled through the exposed skull into the right side and was increased in size using curved mosquito forceps. The final size of the cranial window was obtained using a Kerrison rongeur. Bleeding from the diploe was prevented using bone wax. The dura mater was cut carefully around the edges of the cranial window using microscissors to minimize brain surface injury. The dimensions of the cranial window were ~12×8 mm, with intact arachnoid mater at the base of the window. A stabilization period was maintained before and between SDF recordings. The wound was flushed frequently with sterile 37°C 0.9% saline during this period.

Experimental Groups

Restrictive and Liberal Groups

In the first phase of the study (Fig. 1), the animals were randomized (a computer-generated random list of animals was used) to receive either <2 mL/kg/h fluids (restrictive R group), 0.9% saline was allowed only to flush the intravenous medication, or 30 mL/kg/h (liberal L group) of a balanced isotonic crystalloid solution (Plasmalyte; Baxter SA,

Lessines, Belgium). The first set of brain SDF imaging data and a set of sublingual PBR measurements, as well as hemodynamic and laboratory data, were obtained after infusing the study fluid.

Hypertonic Versus Isotonic Saline Groups

In the second phase of the study (Fig. 1), the animals were randomized (a computer-generated random list of animals was used) to receive 5 mL/kg body weight of either 0.9% saline (group normal saline [NS]) or 3.2% saline (group HTS), administered intravenously over 20 minutes using an infusion pump. The 3.2% saline solution was prepared by the hospital pharmacy. A second set of brain SDF images and a set of sublingual and brain PBR measurements and hemodynamic and laboratory data including syndecan-1 levels were obtained after infusing the study fluid. Hematocrit-corrected serum syndecan-1 levels were calculated according to an equation to compensate for a possible dilution effect of fluids on serum syndecan-1 level: syndecan corrected = syndecan measured × (0.30/measured hematocrit).

The animals were euthanized at the end of the experiment with an overdose of thiopentone (30 mg/kg body weight), and mechanical ventilation was stopped. Syndecan-1 levels were measured using an enzyme-linked immunosorbent assay kit for Syndecan-1 (Blue Gene, Shanghai, China) according to the manufacturer's instructions. The biochemical values were determined by a blood gas analyzer (ABL 800FLEX; Radiometer, Brønshøj, Denmark) and osmometer (Osmometer; Arkray, Tokyo, Japan).

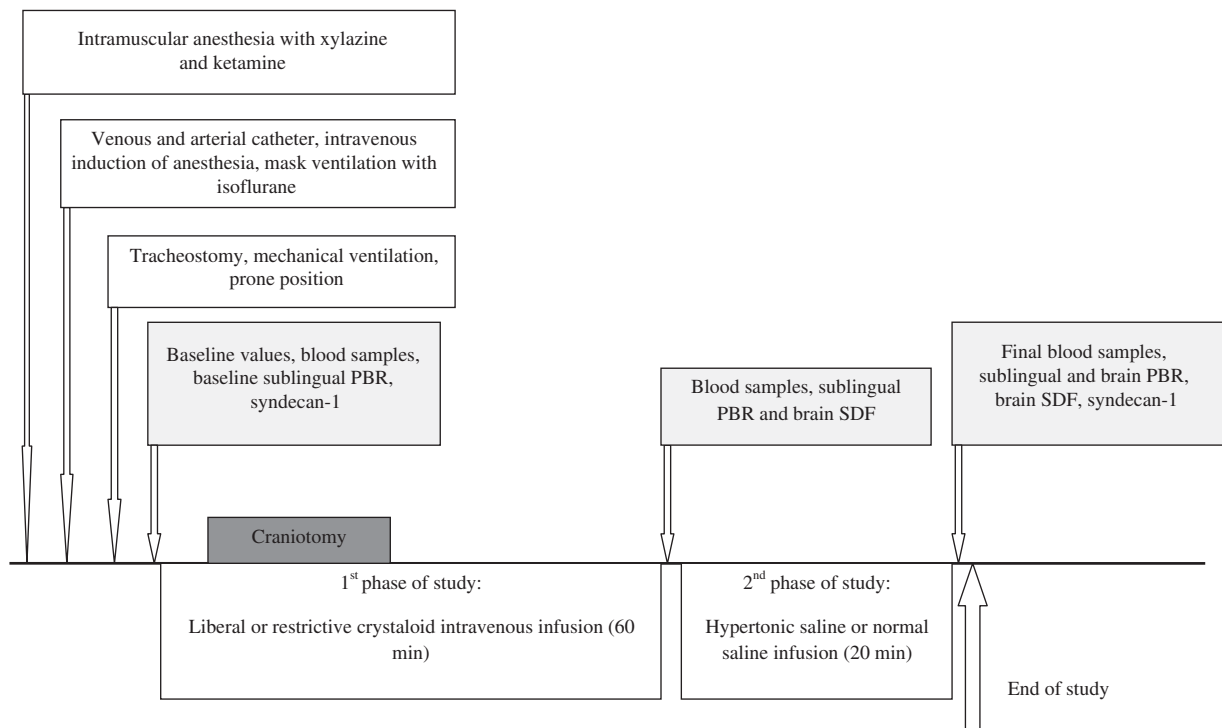


FIGURE 1. Study timeline. PBR indicates perfused boundary region; SDF, sidestream dark-field.

The team members were blinded to the assigned groups while preparing the animals, acquiring data, analyzing the video clips, and conducting the statistical analysis. The administered solution was drawn up offsite and administered by an unblinded coworker (laboratory staff member).

SDF Imaging Procedure

The SDF imaging video microscopic probes were covered with a sterile plastic sheath and placed above the target tissue; a hand-held technique was used. For brain SDF imaging (MicroScan; MicroVision Medical, Amsterdam, the Netherlands), data were recorded digitally within the site of interest on the brain surface for each animal at each measurement, and video clips lasting 20 seconds on average were recorded from each area. A blood flow analysis of larger vessels was used as a control measure, ensuring that excessive pressure was not applied to the tissue.²⁹ The sites of interest in the sublingual area and on the brain surface were selected randomly. The exposed tissues, other than those covered by the SDF imaging probe, were moisturized intermittently using 37°C sterile 0.9% saline.

Videos for the PBR analysis were recorded with a specialized SDF imaging video microscope (KK camera; Research Technology Limited, Honiton, UK) connected to a laptop computer with specialized recording and analysis software (Version 1.2.5.7211; GlycoCheck, Maastricht, the Netherlands). After acquisition, the software performs a series of quality checks to validate that the identified measurement sites reflected the straight segments of the microvessels containing a sufficient number of RBCs, and automatically discards invalid vascular segments and subjects all valid vascular segments to further analysis. Up to 840 radial intensity profiles were obtained for each valid vascular segment, which were tested for the presence of RBCs. RBC filling percentage, signal quality, and RBC column (RBCC) widths were determined from these intensity profiles. This results in an RBC width (RBCW) distribution for each individual vascular segment from which the median RBCW and the outer edge of the RBC-perfused lumen (Dperf) were determined. The distance from the median RBCW value to the outer edge of the RBC-perfused lumen was measured and defined as the PBR (Dperf—RBCW)/2. Finally, the calculated PBR values, classified according to their corresponding RBCC width between 5 and 25 μm , were presented as a single median PBR score for each vessel diameter class, and the corresponding 21 PBR values for diameter classes of 5 to 25 μm were averaged to provide a single PBR value for each measurement.²⁷ This method of calculating the PBR ensures that the average PBR value is equally weighted for each vessel diameter class.^{25–27} A more detailed description of this method is available elsewhere.^{25,27,28} The more the EG is injured, the deeper the RBCs penetrate into the glycocalyx and the higher the PBR.^{9,11,25}

SDF Imaging Offline Analysis

The recorded video clips were randomly coded and analyzed offline by a single observer blinded to the order of the files. The 3 clearest and most stable parts of each video

clip (sequences) meeting the software's stability criteria were selected for analysis. The blood flow in larger vessels was checked to ensure that excessive pressure was not applied during recording. Three sequences per measurement were analyzed from each animal, and the average was used for the calculations. The final onscreen magnification of the images obtained using the SDF imaging device was 325-fold from the original, and the actual size of the field evaluated was 1280×960 μm . The microcirculation parameters were measured using AVA version 3.0 software (AMC, University of Amsterdam, the Netherlands). All analyses were performed by a single, blinded researcher (V.D.Jr) to decrease the probability of interobserver variability.

The following parameters were analyzed offline:

- (1) Total small vessel density (SVD) and total vessel density (TVD) were defined as the total length of the respective vessels inside the image divided by the total area of the image. Small vessels were defined as those with diameters $\leq 25 \mu\text{m}$.²⁹
- (2) The DeBacker score, given in /mm, was defined as the number of vessels crossing 3 arbitrary horizontal and 3 vertical equidistant lines (drawn on the screen) divided by the total length of the lines.²⁹
- (3) The microvascular flow index was calculated as an average value of the semiquantitative score (0=absent flow, 1=intermittent flow, 2=continuous sluggish [slow] flow, 3=continuous [normal] flow, 4=hyperdynamic [fast] flow) of the microvascular flow in the 4 image quadrants, as assessed subjectively by an observer.²⁹
- (4) The proportion of perfused vessels (PPV) was defined as the percentage of all visible vessels with at least sluggish flow. Perfused small vessel density (PSVD) and perfused vessel density (PVD) were obtained as SVD and TVD multiplied by the respective PPVs.

Statistical Analysis

A power analysis using an α error of 0.05 and β error of 0.95 was performed on the basis of our previously published brain microcirculation data for rabbits²³ using G*Power version 3.1.9.2 software (Kiel University, Kiel, Germany). The sample size needed for the *t* test (unmatched pairs) to detect a 20% difference in PVD was calculated. This calculation yielded a sample size of 26 animals (13 subjects/group). The sample size was increased to 28 animals to compensate for potential dropouts and inaccurate predictions used in the power analysis.

The continuous variable results are presented as mean \pm SD or as median with interquartile range on the basis of the results of a normality test of the distribution using the 1-sample Kolmogorov-Smirnov test. Differences in the numbers of animals receiving norepinephrine were analyzed using the Fisher exact test. The Mann-Whitney *U* test was used to compare results between groups, and the Wilcoxon test was used to detect significant changes over time within each group when the sample distribution was not normal (pH, arterial tension of carbon dioxide, arterial tension of oxygen, PPV, microvascular flow index [MFI], hemoglobin, and norepinephrine dose). The

TABLE 1. Hemodynamic and Laboratory Data, Use of Fluids and Catecholamines; Before and After Fluids

| | Baseline | | | After Infusion | | |
|--|---------------------|---------------------|--------|---------------------|---------------------|--------|
| | R Group (n = 14) | L Group (n = 13) | P | R Group (n = 14) | L Group (n = 13) | P |
| MAP (mm Hg) | 66 ± 7 | 68 ± 11 | 0.5172 | 72 ± 13 | 77 ± 23 | 0.5290 |
| Heart rate (beats/min) | 211 ± 29 | 231 ± 32 | 0.0906 | 207 ± 35 | 211 ± 26 | 0.7062 |
| pH | 7.35 (7.33-7.38) | 7.36 (7.35-7.44) | 0.5935 | 7.46 (7.44-7.51)* | 7.46 (7.41-7.52)* | 0.8083 |
| PaCO ₂ (mm Hg) | 50.9 (41.3-55.2) | 50.6 (41.3-55.1) | 0.6623 | 38.7 (35.1-40.7)* | 38.6 (34.1-40.5)* | 0.4969 |
| PaO ₂ (mm Hg) | 156 (129-175) | 149 (92-175) | 0.5281 | 188 (174-197)* | 179 (175-195)* | 0.7524 |
| HCO ₃ ⁻ (mmol/L) | 27.4 ± 2.6 | 27.0 ± 3.6 | 0.7283 | 28.0 ± 2.2 | 26.3 ± 2.9 | 0.0964 |
| Hemoglobin (g/L) | 94.3 ± 6.2 | 92.2 ± 9.3 | 0.5036 | 98.4 ± 6.9* | 89.2 ± 7.8 | 0.0032 |
| Sodium (mmol/L) | 140 (139-141) | 141 (139-142) | 0.4485 | 138 (137-139)* | 140 (139-140) | 0.0080 |
| Chlorides (mmol/L) | 102 ± 4 | 101 ± 5 | 0.5731 | 100 ± 3 | 101 ± 3 | 0.4525 |
| No. animals receiving norepinephrine (N/%) | 11/78.6 | 9/69.3 | 0.6776 | 12/85.7 | 11/84.6 | 1.000 |
| Norepinephrine (mL/h) | 0.600 (0.100-1.000) | 0.200 (0.000-1.775) | 0.8452 | 0.350 (0.100-0.500) | 0.300 (0.100-0.550) | 0.9806 |
| Sublingual PBR (µm) | 1.93 ± 0.26 | 2.00 ± 0.22 | 0.5808 | 2.05 ± 0.21 | 2.02 ± 0.26 | 0.8082 |

Continuous data are presented as mean ± SD or as median (IQR) based on the results of the Kolmogorov-Smirnov test. Categorical data are given as counts/percentages. HCO₃⁻ indicates actual bicarbonate; L group, liberal group; MAP, mean arterial pressure; PaCO₂, arterial tension of carbon dioxide, PaO₂, arterial tension of oxygen; PBR, perfused boundary region; R group, restrictive group.
*P < 0.05 versus baseline.

unpaired 2-tailed *t* test was used to compare all other results between the groups; the paired 2-tailed *t* test or 1-way analysis of variance with the Student-Newman-Keuls test for pairwise comparisons was used to compare other results within the groups. One-way analysis of variance with the Student-Newman-Keuls test for pairwise comparisons of subgroups and the Kruskal-Wallis test were used to compare results between subgroups on the basis of the results of normality testing. Uncorrected *P*-values are presented, and a *P* < 0.05 was considered significant. The statistical analysis was performed using MedCalc Statistical Software version 16.4.3 (MedCalc Software, Ostend, Belgium; https://www.medcalc.org; 2018).

RESULTS

One animal died during the instrumentation phase, and 27 animals completed the first part of the study (14 in the R group and 13 in the L group). No differences were observed in weight (2.96 ± 0.24 vs. 2.87 ± 0.24 kg; *P* = 0.940) or initial hemodynamic and laboratory data between the groups (Table 1).

Fluid intake was significantly higher in the L group than in the R group (86.9 ± 8.3 vs. 6.2 ± 3.2 mL; *P* < 0.0001). After administering fluids, a higher hemoglobin value and a lower sodium value were recorded in the R group compared with the L group (Table 1). No difference was observed between the animals receiving norepinephrine and those not receiving norepinephrine. No differences in sublingual PBR values were observed before and after fluid administration (Table 1).

Table 2 lists the cortical brain microcirculation parameters obtained after fluid administration. Lower TVD (*P* = 0.0447), PSVD (*P* = 0.0178), and PVD (*P* = 0.0286) values were observed in the L group than in the R group.

In total, 27 animals completed the second phase of the study (14 HTS and 13 NS). The volume of fluid administered during the first phase of the study was similar in the HTS and NS groups, 41.0 (6.0; 94.0) versus 14.0 (5.8; 82.8) mL, respectively (*P* = 0.6448).

Table 3 compares the hemodynamic data and laboratory values as well as administered fluids, catecholamines, and sublingual PBR before and after osmotherapy. Higher serum osmolality, and sodium and chloride levels were observed after osmotherapy in the HTS group compared with the NS group. Lower pH values were recorded in both groups, as well as higher arterial tension of carbon dioxide and lower chloride levels in the NS group, but lower bicarbonate and higher sodium and chloride levels were observed in the HTS group after osmotherapy. No differences were observed in the hemodynamic data, the use of catecholamines, or sublingual PBR between the groups before or after osmotherapy.

Table 4 lists the cortical brain microcirculation parameters and brain PBR values obtained before and after osmotherapy. MFI values were lower in the HTS group than in the NR group before and after osmotherapy. No other difference was recorded in the observed microcirculation parameters.

After osmotherapy, serum syndecan-1 levels (1.37 ± 0.51 vs. 1.24 ± 0.39 ng/mL; *P* = 0.5174) were not different between

TABLE 2. Brain Microcirculation Parameters After Fluids

| | R Group (n = 14) | L Group (n = 13) | P |
|----------------------------|--------------------|-------------------|--------|
| SVD (mm/mm ²) | 7.36 ± 1.48 | 6.27 ± 1.33 | 0.0816 |
| TVD (mm/mm ²) | 9.85 ± 1.37 | 8.79 ± 0.96 | 0.0447 |
| PSVD (mm/mm ²) | 7.20 ± 1.38 | 5.83 ± 1.16 | 0.0178 |
| PVD (mm/mm ²) | 9.70 ± 1.37 | 8.40 ± 1.27 | 0.0286 |
| PPV (%) | 100.0 (98.6-100.0) | 98.4 (86.2-100.0) | 0.2037 |
| MFI small vessels | 3.0 (3.0-3.0) | 3.0 (2.9-3.0) | 0.3851 |
| DeBacker score (/mm) | 6.44 ± 1.2 | 5.77 ± 0.48 | 0.1172 |
| DeBacker grid crossings | 24.4 ± 5.0 | 21.4 ± 2.2 | 0.0796 |

Continuous data are presented as mean ± SD or as median (IQR) based on the results of the Kolmogorov-Smirnov test.
L group indicates liberal group; MFI, microvascular flow index; PPV, proportion of perfused vessels; PSVD, perfused small vessel density; PVD, perfused vessel density; R group, restrictive group; SVD, small vessel density; TVD, total vessel density.

TABLE 3. Hemodynamic and Laboratory Data, Use of Fluids, Catecholamines, Sublingual PBR After NS or HTS

| | Before Osmotherapy | | | After Osmotherapy | | |
|--|--------------------|-------------------|--------|--------------------|-------------------|----------|
| | HTS Group (n = 14) | NS Group (n = 13) | P | HTS Group (n = 14) | NS Group (n = 13) | P |
| MAP (mm Hg) | 71.9 ± 13.2 | 76.5 ± 12.3 | 0.0530 | 71.8 ± 16.7 | 75.2 ± 10.5 | 0.5395 |
| Heart rate (beats/min) | 207 ± 35 | 211 ± 25 | 0.2800 | 200 ± 36 | 199 ± 27 | 0.9461 |
| pH | 7.45 (7.41-7.51) | 7.48 (7.44-7.52) | 0.2541 | 7.41 (7.38-7.47)* | 7.42 (7.40-7.49)* | 0.7203 |
| PaCO ₂ (mm Hg) | 39.4 (35.1-44.9) | 37.8 (33.7-39.4) | 0.0900 | 40.5 (37.5-45.1) | 42.1 (39.1-44.9)* | 0.4667 |
| PaO ₂ (mm Hg) | 186 (178-197) | 178 (172-194) | 0.1742 | 183 (170-188) | 176 (160-186) | 0.5441 |
| HCO ₃ ⁻ (mmol/L) | 27.3 ± 2.7 | 27.0 ± 2.6 | 0.7298 | 26.1 ± 2.5* | 26.9 ± 4.3 | 0.5834 |
| Hemoglobin (g/L) | 92.0 (91.0-101.0) | 94.0 (88.8-99.0) | 0.7339 | 91.5 (87.0-94.0)* | 93.0 (88.5-103.3) | 0.2069 |
| Sodium (mmol/L) | 139 ± 2 | 139 ± 2 | 0.8388 | 143 ± 2* | 138 ± 1 | < 0.0001 |
| Chlorides (mmol/L) | 100 (99-102) | 100 (99-102) | 0.7890 | 107 (105-108)* | 99 (97-102)* | < 0.0001 |
| Serum osmolality (mmol/kg) | — | — | — | 302 (300-304) | 292 (290-295) | 0.0004 |
| No. animals receiving norepinephrine (N/%) | 13/92.9 | 11/84.6 | 0.5956 | 13/92.9 | 13/100 | 1.0000 |
| Norepinephrine (mL/h) | 0.45 (0.30-0.70) | 0.20 (0.10-0.43) | 0.0840 | 0.50 (0.40-0.80) | 0.50 (0.20-0.73) | 0.5597 |
| Sublingual PBR (µm) | 2.04 ± 0.23 | 2.04 ± 0.26 | 0.9893 | 1.88 ± 0.54 | 1.92 ± 0.24 | 0.8177 |

Continuous data are presented as mean ± SD or as median (IQR) based on the results of the Kolmogorov-Smirnov test. Categorical data are given as counts/percentages. HCO₃⁻ indicates actual bicarbonate; HTS, hypertonic saline; MAP, mean arterial pressure; NS, normal saline; PaCO₂, arterial tension of carbon dioxide; PaO₂, arterial tension of oxygen; PBR, perfused boundary region.

*P < 0.05 versus before osmotherapy.

the HTS and NS groups or from baseline values (1.29 ± 0.29 vs. 1.05 ± 0.39 ng/mL; P = 0.1032). Hematocrit-corrected serum syndecan-1 levels were also not different between the HTS and NS groups (1.43 ± 0.60 vs. 1.36 ± 0.49 ng/mL; P = 0.7372) or from baseline values.

Table 5 lists the cortical brain microcirculation parameters, and brain and sublingual PBR and serum syndecan-1 levels in the 4 animal subgroups divided according to osmotherapy and infusion strategy. No significant difference was detected between the subgroups.

A subgroup analysis of animals receiving liberal fluid loading (animals from subgroups liberal with normal saline [LNS] and liberal with hypertonic saline [LHTS]) showed a tendency for slightly higher syndecan-1 levels (1.47 ± 0.51 vs. 1.16 ± 0.35 ng/mL; P = 0.0993) compared with animals receiving restricted fluid infusion (animals from subgroups RNS and RHTS). This difference was significant if serum hematocrit-corrected syndecan-1 levels were considered (1.64 ± 0.63 vs. 1.16 ± 0.31 ng/mL; P = 0.0324).

Sublingual and cerebral PBR values after fluids and osmotherapy were not different (1.90 ± 0.41 vs. 1.89 ± 0.33

µm; P = 0.9440). No significant differences were observed in the sublingual PBR values between animals from the liberal fluid loading and restrictive fluid subgroups (1.86 ± 0.57 vs. 1.94 ± 0.26 µm; P = 0.5763).

Cerebral PBR values tended to be higher in animals from the liberal fluid loading and restrictive fluid subgroups (2.04 ± 0.33 vs. 1.77 ± 0.28 µm; P = 0.0692, respectively). A significant difference (Fig. 2) was identified in the range of RBCC widths between 20 and 25 µm (1.76 ± 0.27 vs. 2.39 ± 0.61 µm; P = 0.0066).

DISCUSSION

In this study, we observed that liberal fluid loading with an isotonic balanced crystalloid solution was associated with altered cerebral cortex microcirculation compared with a restrictive infusion strategy, whereas the use of HTS did not alter cerebral cortex microcirculation in the animal craniotomy model.

Fluid loading can alter cerebral cortex microcirculation through several mechanisms. Intravenous crystalloid solution

TABLE 4. Brain Microcirculation Parameters and Cortical Brain PBR Before and After Osmotherapy

| | Before Osmotherapy | | | After Osmotherapy | | |
|----------------------------|--------------------|--------------------|--------|--------------------|--------------------|--------|
| | HTS Group (n = 14) | NS Group (n = 13) | P | HTS Group (n = 14) | NS Group (n = 13) | P |
| SVD (mm/mm ²) | 6.76 ± 1.51 | 6.93 ± 1.53 | 0.7933 | 6.69 ± 1.42 | 7.16 ± 1.74 | 0.4606 |
| TVD (mm/mm ²) | 9.15 ± 1.18 | 9.56 ± 1.42 | 0.4553 | 9.13 ± 0.78 | 9.44 ± 1.77 | 0.5789 |
| PSVD (mm/mm ²) | 6.26 ± 1.36 | 6.85 ± 1.51 | 0.3308 | 6.56 ± 1.39 | 6.90 ± 1.59 | 0.5713 |
| PVD (mm/mm ²) | 8.70 ± 1.44 | 9.49 ± 1.41 | 0.2008 | 8.93 ± 0.64 | 9.19 ± 1.79 | 0.6370 |
| PPV (%) | 98.5 (85.72-100.0) | 100.0 (98.7-100.0) | 0.1102 | 98.9 (97.5-100.0) | 100.0 (97.4-100.0) | 0.8052 |
| MFI | 3.0 (2.8-3.0) | 3.0 (3.0-3.0) | 0.0106 | 3.0 (3.0-3.0) | 3.00 (2.9-3.00) | 0.0326 |
| DeBacker score (mm) | 5.95 ± 0.65 | 6.30 ± 1.32 | 0.4482 | 5.91 ± 0.68 | 6.17 ± 1.24 | 0.5221 |
| DeBacker grid crossings | 22.1 ± 2.9 | 23.9 ± 5.1 | 0.2858 | 22.4 ± 2.6 | 23.4 ± 4.8 | 0.5146 |
| PBR brain (µm) | — | — | — | 1.88 ± 0.31 | 1.90 ± 0.35 | 0.9284 |

Continuous data are presented as mean ± SD or as median (IQR) based on results of Kolmogorov-Smirnov test.

HTS indicates hypertonic saline; MFI, microvascular flow index; NS, normal saline; PBR, perfused boundary region; PPV, proportion of perfused vessels; PSVD, perfused small vessel density; PVD, perfused vessel density; SVD, small vessel density; TVD, total vessel density.

TABLE 5. Brain Microcirculation Parameters and Syndecan-1 Levels After Fluids and Osmotherapy—Subgroups

| | LHTS Subgroup (n = 7) | LNS Subgroup (n = 6) | RHTS Subgroup (n = 7) | RNS Subgroup (n = 7) | P |
|---------------------------------|-----------------------|----------------------|-----------------------|----------------------|--------|
| SVD (mm/mm ²) | 6.62 ± 1.56 | 6.80 ± 1.29 | 7.78 ± 1.87 | 6.59 ± 1.63 | 0.8847 |
| TVD (mm/mm ²) | 8.96 ± 2.13 | 9.08 ± 0.66 | 10.00 ± 1.18 | 9.18 ± 0.92 | 0.5472 |
| PSVD (mm/mm ²) | 6.50 ± 1.64 | 6.72 ± 1.25 | 7.36 ± 1.55 | 6.42 ± 1.58 | 0.6950 |
| PVD (mm/mm ²) | 8.86 ± 2.22 | 8.91 ± 0.56 | 9.57 ± 1.19 | 8.96 ± 0.75 | 0.7821 |
| PPV (%) | 100 (98.9-100.0) | 99.5 (98.9-100.0) | 98.9 (96.3-100.0) | 98.6 (96.5-100.0) | 0.8417 |
| MFI | 2.96 (2.89-3.00) | 3.00 (3.00-3.00) | 3 (2.83-3.00) | 3.00 (3.00-3.00) | 0.1349 |
| DeBacker score (/mm) | 5.83 (4.70-6.79) | 5.89 (5.75-6.09) | 6.14 (6.08-6.76) | 6.11 (4.96-6.50) | 0.4798 |
| DeBacker grid crossings | 22.3 (17.8-23.0) | 22.7 (21.3-23.0) | 23.3 (23.3-25.0) | 23.7 (19.1-24.7) | 0.5150 |
| PBR brain (µm) | 1.95 ± 0.38 | 2.21 ± 0.07 | 1.84 ± 0.35 | 1.72 ± 0.23 | 0.1774 |
| PBR sublingual (µm) | 1.71 ± 0.73 | 2.02 ± 0.26 | 2.03 ± 0.27 | 1.85 ± 0.22 | 0.4912 |
| Syndecan-1 (ng/mL) | 1.55 ± 0.58 | 1.37 ± 0.42 | 1.20 ± 0.38 | 1.08 ± 0.32 | 0.3633 |
| Syndecan-1 Ht corrected (ng/mL) | 1.71 ± 0.71 | 1.53 ± 0.55 | 1.17 ± 0.31 | 1.13 ± 0.39 | 0.1968 |

Continuous data are presented as mean ± SD or as median (IQR) based on the results of the Kolmogorov-Smirnov test. Ht indicates hematocrit; LHTS, liberal with hypertonic saline; LNS, liberal with normal saline; MFI, microvascular flow index; PBR, perfused boundary region; PPV, proportion of perfused vessels; PSVD, perfused small vessel density; PVD, perfused vessel density; RHTS, restrictive with hypertonic saline; RNS, restrictive with normal saline; SVD, small vessel density; TVD, total vessel density.

leaves the blood vessels and is distributed in the extracellular volume causing edema. It is generally accepted that plasma osmolality is the key determinant of water movement between the central nervous system and the intravascular space in the presence of an intact BBB.³⁰ Available data indicate that volume replacement and expansion should have no effect on cerebral edema as long as normal serum osmolality is maintained and cerebral hydrostatic pressure does not increase markedly due to a true volume overload and elevated right heart pressure.³¹ If the BBB is disrupted, brain capillaries will be likely to act more like peripheral capillaries. A blunt or penetrating injury incites mechanical and autodigestive destruction of the normally tightly intact endothelium of the BBB,³² allowing for uncontrolled movement of fluid and serum proteins into the brain parenchyma, and eventually leading to vasogenic cerebral edema and increased intracranial pressure (ICP). The combined effect of fluid overload and

altered BBB tightness due to a minor mechanical injury to the brain surface during the instrumentation phase seems to be the most probable explanation for our observation.

Aggressive fluid administration can be associated with volume overload,³³ which could, in turn, be linked to venous congestion and a decline in cardiac output in subjects with heart failure.³⁴ Increased central venous pressure may impede brain venous outflow and contribute to increased ICP or cerebral edema.³ We performed an extensive craniotomy to measure microcirculation; therefore, we do not consider an increase in ICP as an alteration mechanism of microcirculation in the liberal group. We did not measure central venous pressure, cerebral perfusion pressure, or cerebral blood flow; therefore, we cannot fully exclude the effects of these mechanisms.

Tonicity changes may also be important, as hypotonic fluids promote water shifts in the brain, because the BBB is water permeable, whereas hypertonic fluids cause brain dehydration, when the BBB is intact or disrupted.³⁵ The solution used in this study had an osmolality of 295 mOsm/L, which should have prevented any changes in osmolality and increased brain water content under normal conditions.³⁶ Although osmolality was not directly measured after fluid administration, lower serum sodium levels in the R group and similar serum levels of bicarbonate and chloride observed in both groups do not support this mechanism of action.

Acute volume overload can modify sympathetic tone and vasoconstriction; however, this response has only been described in renal circulation after massive 0.9% saline infusion leading to hypernatremia and hyperchloremic metabolic acidosis.^{37,38} We did not observe any significant difference in the use of norepinephrine, circulatory parameters, or sodium or chloride levels between the groups after fluid administration that could imply the effects of these mechanisms.

Lung function complications associated with fluid overload can be associated with reduced lung compliance and altered oxygen or carbon dioxide levels in arterial blood³⁹; however, our data do not support this event.

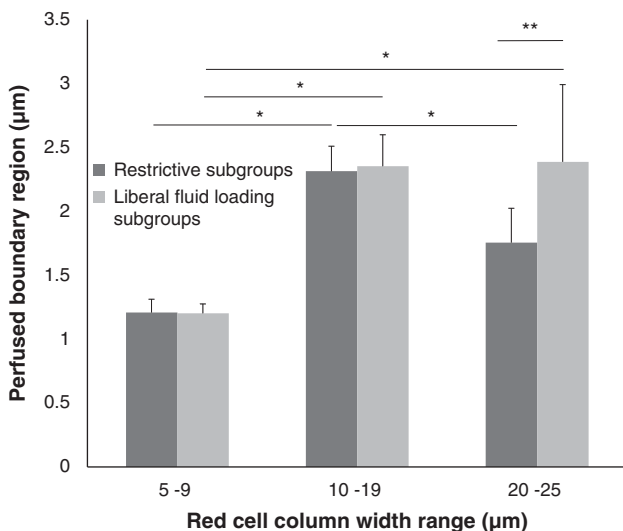


FIGURE 2. Microvascular perfused boundary region according to the red blood cell column width range. *P < 0.05; **P < 0.01.

Normovolemic hemodilution can also decrease blood viscosity and blood oxygen content, and increase cerebral blood flow under experimental conditions. These changes, which are probably dependent on reduced blood oxygen content,⁴⁰ are contrary to our observations. We observed lower hemoglobin levels under a liberal infusion strategy, as expected; however, better microcirculation parameters were observed in the R infusion group.

The extent of the difference in the microcirculatory parameters between the R and the L groups ranged from ~9% for TVD, to 15% and 20% for PVD and PSVD, respectively. The clinical significance of these differences is unclear. A similar, although nonsignificant difference in PVD values, and no change in the MFI or PPV values, were observed when comparing microcirculation in “pericontusional” with “surrounding” cortical brain areas in patients with traumatic brain injury.⁴¹ A different finding was observed in patients undergoing decompressive craniectomy after an ischemic stroke.⁴² In that study, the PPVs was near 100% in control subjects and only 63.44% in patients with stroke. Patients with stroke also presented intermittent or no flow in all vessels. The PVD index was <50% of the control value.

Importantly, the liberal use of crystalloids was accompanied by altered EG structure, as implied by hematocrit-corrected serum syndecan-1 levels. The EG acts as an anionic biopolymer with specific ion-binding properties.⁴³ Volume loading may release an excess of the atrial natriuretic factor associated with increased shedding of the EG, as recently described after a 20 mL/kg infusion of 6% hydroxyethyl starch 130/0.4 in patients undergoing elective surgery.¹³ Similar results were replicated in patients undergoing elective laparoscopic surgery who received 15 mL/kg/h of Ringer’s solution intraoperatively and 10 mL/kg/h for 6 hours postoperatively.⁴⁴ The dose of crystalloids used in our study corresponded to ~12% of the rabbit extracellular fluid volume.⁴⁵ The equivalent change in human extracellular fluid volume would be obtained by ~20 mL/kg of isotonic crystalloid solution.

The use of a hyperosmolar solution can alter cerebral microcirculation by several mechanisms. The short-term effects of 3.2% saline, 0.5 M sodium lactate, and 0.9% saline solutions were recently studied using SDF imaging technology in a rabbit craniotomy model by our group.²⁴ No differences in the microcirculatory parameters were observed between the groups after osmotherapy.

Ambient sodium overload may also alter the glycocalyx structure, probably due to reduced heparan sulfate content leading to collapse of the EG.¹⁴ Hypertonic solutions also modify microvascular permeability and show a dose-dependent effect on hydraulic permeability as a measure of water flow across the endothelial barrier in the mesenteric vessels of rats.⁴⁶ Such an increase in vascular permeability has been considered an indirect sign of EG damage. Moreover, sodium flux into endothelial cells triggers intracellular signaling and influences endothelial function as long as intracellular aldosterone receptors are

functional.^{47,48} Glycocalyx shedding allows sodium to enter into the endothelial cells and subsequently disturb endothelial function. Thus, high sodium levels may weaken the protective sodium buffer barrier of the EG. Increased osmolality may also contribute to glycocalyx shedding⁴⁹; however, our results disagree with these observations, possibly due to the limited change of osmolality in our experimental model. In addition, the time factor could also have affected our results, given the limited observation period.

Although we found elevated hematocrit-corrected syndecan-1 levels in the L fluid-loaded animals, this finding was accompanied with only a nonsignificant trend toward higher cerebral PBR values, and significantly lower PBR values were recorded only in the 20 to 25 μ m range of RBCC diameters in the L fluid-loaded animals. The lower PBR value in larger vessels contrasts with recent findings, implying that PBR values reach a plateau from an RBCC width of 15 μ m upwards.²⁸ Our finding could possibly be a result of lower shear stress in arterioles in the R group,¹⁰ but the finding could also be a consequence of a technical limitation of the method. The glycocalyx is determined by RBCC width variation during SDF imaging.^{9,10,25,27} SDF imaging is prone to motion and pressure artifacts, similar to orthogonal polarization spectral imaging. Motion-induced image blurring due to movement of the SDF device and the tissue, and flow of erythrocytes, can cause suboptimal imaging.⁹ It has recently been shown that pressure artifacts caused by a sterile slipcover influences the PBR values obtained.²⁸ In contrast to that human study, we did not observe significantly different PBR values in cortical and sublingual regions. Our results imply that PBR may be less sensitive or more operator dependent than the use of biochemical markers of EG damage.

Our study had several limitations. The absence of a baseline brain SDF examination before fluid loading weakened the strength of our conclusion on the effect of fluid loading on brain microcirculation. The use of fluid loading in the first phase of the study caused large intragroup differences that might make significant changes in the second phase undetectable. This study had insufficient power to test differences in PBR and serum syndecan-1 levels between the subgroups. A higher number of animals may have resulted in a greater difference between the groups and a decreased risk of false-positive or false-negative results. We did not directly measure BBB permeability; therefore, our conclusions on the mechanism of altered microcirculation after fluid loading remain speculative. We visualized only pial vessels and the frontal cortex; however, these areas may not be representative of deeper brain structures. The PBR analysis has not been validated in the cerebral cortex or in rabbits. To limit brain surface injury, changes in microcirculation were evaluated only at predefined timepoints; therefore, we cannot exclude the possibility that the observed effects may have been different if other timepoints had been chosen. We also used rabbit brain, which has unknown similarities in blood flow regulation to those of the human

brain. Therefore, it is unclear whether our results can be safely extrapolated to humans.

CONCLUSIONS

Within the limitations of the present study, our findings imply that L fluid loading was associated with altered cortical cerebral microcirculation and elevated markers of EG integrity compared with the R infusion strategy in the rabbit craniotomy model. The use of a single bolus of 3.2% saline did not affect cortical cerebral microcirculation or markers of EG integrity.

REFERENCES

- Doherty M, Buggy GJ. Intraoperative fluids: how much is too much. *Br J Anaesth*. 2012;109:69–79.
- Lilot M, Ehrenfeld JM, Lee C, et al. Variability in practice and factors predictive of total crystalloid administration during abdominal surgery: retrospective two-centre analysis. *Br J Anaesth*. 2015;114:767–776.
- Van der Jagt M. Fluid management of the neurological patient: a concise review. *Crit Care*. 2016;20:126.
- Luo J, Xue J, Liu J, et al. Goal-directed fluid restriction during brain surgery: a prospective randomized controlled trial. *Ann Intensive Care*. 2017;7:16.
- Kayilioglu SI, Dinc T, Sozen I, et al. Postoperative fluid management. *World J Crit Care Med*. 2015;4:192–201.
- Iadecola C. Neurovascular regulation in the normal brain and in Alzheimer's disease. *Nat Rev Neurosci*. 2004;5:347–360.
- Abbott NJ, Patabendige AAK, Dolman DEM, et al. Structure and function of the blood-brain barrier. *Neurobiol Dis*. 2010;37:13–25.
- Jacob M, Chappell D, Becker B. Regulation of blood flow and volume exchange across the microcirculation. *Crit Care*. 2016;20:319.
- Haeren RH, van de Ven SE, van Zandvoort MA, et al. Assessment and imaging of the cerebrovascular glycocalyx. *Curr Neurovasc Res*. 2016;13:249–260.
- Reitsma S, Slaaf DW, Vink H, et al. The endothelial glycocalyx: composition, functions, and visualization. *Pflugers Arch*. 2007;454:345–359.
- Cerny V, Astapenko D, Brettner F, et al. Targeting the endothelial glycocalyx in acute critical illness as a challenge for clinical and laboratory medicine. *Crit Rev Clin Lab Sci*. 2017;54:343–357.
- Zhu J, Li X, Yin J, et al. Glycocalyx degradation leads to blood-brain barrier dysfunction and brain edema after asphyxia cardiac arrest in rats. *J Cereb Blood Flow Metab*. 2017;27:1678X17726062. [Epub ahead of print].
- Chappell D, Bruegger D, Potzel J, et al. Hypervolemia increases release of atrial natriuretic peptide and shedding of the endothelial glycocalyx. *Crit Care*. 2014;18:538.
- Oberleithner H, Peters W, Kusche-Vihrog K, et al. Salt overload damages the glycocalyx sodium barrier of vascular endothelium. *Pflugers Arch*. 2011;462:519–528.
- Schierke F, Wyrwoll MJ, Wisdorf M, et al. Nanomechanics of the endothelial glycocalyx contribute to Na⁺-induced vascular inflammation. *Sci Rep*. 2017;7:46476.
- Goedhart PT, Khalilzade M, Bezemer R, et al. Sidestream dark field (SDF) imaging: a novel stroboscopic LED ring-based imaging modality for clinical assessment of the microcirculation. *Opt Express*. 2007;15:15101–15114.
- Bartels SA, Bezemer R, Milstein DM, et al. The microcirculatory response to compensated hypovolemia in a lower body negative pressure model. *Microvasc Res*. 2011;82:374–380.
- de Backer D, Creteur J, Dubois MJ, et al. Microvascular alterations in patients with severe heart failure and cardiogenic shock. *Am Heart J*. 2004;147:91–99.
- Sitina M, Turek Z, Parizkova R, et al. In situ assessment of the brain microcirculation in mechanically-ventilated rabbits using sidestream dark-field (SDF) imaging. *Physiol Res*. 2011;60:75–81.
- Sitina M, Turek Z, Parizkova R, et al. Preserved cerebral microcirculation in early stages of endotoxemia in mechanically-ventilated rabbits. *Clin Hemorheol Microcirc*. 2011;47:37–44.
- Taccone FS, Su F, Pierrakos C, et al. Cerebral microcirculation is impaired during sepsis: an experimental study. *Crit Care*. 2010;14:R140.
- Taccone FS, Su F, De Deyne C, et al. Sepsis is associated with altered cerebral microcirculation and tissue hypoxia in experimental peritonitis. *Crit Care Med*. 2014;42:e114–e122.
- Dostal P, Schreiberova J, Dostalova V, et al. Effects of hypertonic saline and mannitol on cortical cerebral microcirculation in a rabbit craniotomy model. *BMC Anesthesiol*. 2015;15:88.
- Dostalova V, Schreiberova J, Dostalova V Jr, et al. Effects of hypertonic saline and sodium lactate on cortical cerebral microcirculation and brain tissue oxygenation. *J Neurosurg Anesthesiol*. 2018;30:163–170.
- Lee DH, Dane MJ, van den Berg BM, et al. Deeper penetration of erythrocytes into the endothelial glycocalyx is associated with impaired microvascular perfusion. *PLoS One*. 2014;9:e96477.
- Dane MJ, Khairoun M, Lee DH, et al. Association of kidney function with changes in the endothelial surface layer. *Clin J Am Soc Nephrol*. 2014;9:698–704.
- Rovas A, Lukasz A-H, Vink H, et al. Bedside analysis of the sublingual microvascular glycocalyx in the emergency room and intensive care unit—the GlycoNurse study. *Scand J Trauma Resusc Emerg Med*. 2018;26:16.
- Haeren RHL, Rijkers K, Schijns OEMG, et al. In vivo assessment of the human cerebral microcirculation and its glycocalyx: a technical report. *J Neurosci Method*. 2018;303:114–125.
- De Backer D, Hollenberg S, Boerma C, et al. How to evaluate the microcirculation? Report of a round table conference. *Crit Care*. 2007;11:R101.
- Hladky SB, Barrand MA. Mechanisms of fluid movement into, through and out of the brain: evaluation of the evidence. *Fluids Barriers CNS*. 2014;11:26.
- Alvis-Miranda HR, Castellar-Leones SM, Moscote-Salazar LR. Intravenous fluid therapy in traumatic brain injury and decompressive craniectomy. *Bull Emerg Trauma*. 2014;2:3–14.
- Werner C, Engelhard K. Pathophysiology of traumatic brain injury. *Br J Anaesth*. 2007;99:4–9.
- Ogbu OC, Murphy DJ, Martin GS. How to avoid fluid overload. *Curr Opin Crit Care*. 2015;21:315–321.
- Miller WL. Fluid volume overload and congestion in heart failure: time to reconsider pathophysiology and how volume is assessed. *Circ Heart Fail*. 2016;9:e002922.
- Shackford SR, Zhuang J, Schmoker J. Intravenous fluid tonicity: effect on intracranial pressure, cerebral blood flow, and cerebral oxygen delivery in focal brain injury. *J Neurosurg*. 1992;76:91–98.
- Tommasino C, Picozzi V. Volume and electrolyte management. *Best Pract Res Clin Anaesthesiol*. 2007;21:497–516.
- Lira A, Pinsky MR. Choices in fluid type and volume during resuscitation: impact on patient outcomes. *Ann Intensive Care*. 2014;4:38.
- Chowdhury AH, Cox EF, Francis ST, et al. A randomized, controlled, double-blind crossover study on the effects of 2-L infusion of 0.9% saline and Plasma-Lyte(R) 148 on renal blood flow velocity and renal cortical tissue perfusion in healthy volunteers. *Ann Surg*. 2012;256:18–24.
- Claude-Del Granado R, Mehta RL. Fluid overload in the ICU: evaluation and management. *BMC Nephrology*. 2016;17:109.
- Tomiya Y, Jansen K, Brian JE Jr, et al. Hemodilution, cerebral O₂ delivery, and cerebral blood flow: a study using hyperbaric oxygenation. *Am J Physiol*. 1999;276:H1190–H1196.
- Pérez-Bárcena J, Romay E, Llompert-Pou JA, et al. Direct observation during surgery shows preservation of cerebral microcirculation in patients with traumatic brain injury. *J Neurol Sci*. 2015;353:38–43.
- Pérez-Bárcena J, Goedhart P, Ibáñez J, et al. Direct observation of human microcirculation during decompressive craniectomy after stroke. *Crit Care Med*. 2011;39:1126–1129.
- Siegel G, Walter A, Kauschmann A, et al. Anionic biopolymers as blood flow sensors. *Biosens Bioelectron*. 1996;11:281–294.

44. Belavić M, Sotošek Tokmadžić V, Fišić E, et al. The effect of various doses of infusion solutions on the endothelial glycocalyx layer in laparoscopic cholecystectomy patients. *Minerva Anesthesiol.* 2018. Doi:10.23736/S0375-9393.18.12150-X. [Epub ahead of print].
45. Davies B, Morris T. Physiological parameters in laboratory animals and humans. *Pharm Res.* 1993;10:1093–1095.
46. Victorino GP, Newton CR, Curran B. Effect of hypertonic saline on microvascular permeability in the activated endothelium. *J Surg Res.* 2003;112:79–83.
47. Oberleithner H, Riethmüller C, Schillers H, et al. Plasma sodium stiffens vascular endothelium and reduces nitric oxide release. *Proc Natl Acad Sci U S A.* 2007;104:16281–16286.
48. Oberleithner H, Wälte M, Kusche-Vihrog K. Sodium renders endothelial cells sticky for red blood cells. *Front Physiol.* 2015;6:188.
49. Genét GF, Bentzer P, Ostrowski SR, et al. Resuscitation with pooled and pathogen-reduced plasma attenuates the increase in brain water content following traumatic brain injury and hemorrhagic shock in rats. *J Neurotrauma.* 2017;34:1054–1062.